INSTITUTO ARGENTINO DEL PETROLEO Y DEL GAS

NEW GENERATION 3D SIMULATOR PREDICTS REALISTIC MUD DISPLACEMENT IN HIGHLY DEVIATED AND HORIZONTAL WELLS

S. P. Baggini Almagro, Schlumberger SAlmagro@slb.com, N.C. Flamant, Schlumberger NFlamant@slb.com and C. Sri Sutama, Schlumberger CSutama@slb.com

Abstract

Effective mud removal is a prerequisite to attain the cement coverage necessary for good zonal isolation. Because of this, the oilfield industry has dedicated considerable attention to the topic of mud displacement over the past 60 years. The first 2D annular displacement simulator was introduced in the 1990s and it is now widely available. The results are satisfactory for simpler configurations. However, for deeper wells with complex trajectories such as highly deviated or horizontal wells, the models start to show their limits. This paper discusses the advancements in mud displacement simulation that overcome the limitations of the previous generation simulator and provide a more realistic simulation in highly deviated and horizontal wells.

A new generation simulator now provides high-fidelity results via a combination of: 1) a pipe displacement model, accounting for fluid contamination inside the pipe; 2) a high-resolution annular displacement model, accounting for the complex 3D annulus shape with full determination of axial and azimuthal flows; and 3) a stiff-string centralization model based on the finite-element method, predicting casing position in a 3D wellbore.

A primary cementing operation for a horizontal well was studied and an unprecedented congruence was witnessed between predicted fluids annular concentration maps and ultrasonic cement log. The simulator was also able to predict complex channeling patterns in the annulus. These results allow a better understanding of the cement placement technique and provide means to optimize the sequence of fluids to achieve effective mud displacement in the well.

Enabled by advancements in today’s computing capabilities, the new simulator is able to simulate both simple and highly complex scenarios more realistically. Finally, the new model allows better planning and decision making to achieve zonal isolation and well objectives.

Introduction

The main objective of a primary cementing job is to provide complete and permanent isolation of the formation behind casing, so that the well can be operated safely and economically. To meet this objective, the annular space must be completely filled with cement slurry. Drilling mud (and any other fluids pumped before cement) must be fully removed from the annulus.

Because of this criticality, mud displacement has always been an important subject in the oil and gas cementing domain. As early as 1940, using a large-scale simulator, (Jones & Berdine, 1940) had investigated the factors influencing oil-well cementing failures, including channeling of cement slurry and the presence of mud cake. They proposed several methods to improve cement placement: casing centralization, casing movement, water circulation prior to cement, and the use of mechanical devices.

However, they acknowledged that the results from these techniques could not be assessed quantitatively, and that their conclusions were based largely on visual observations.

Since those early days, many studies have been performed to better understand mud displacement. (McLean, Manry, & Whitaker, 1967) developed an analytical model based on laboratory experiments, (Zuiderwijk, 1974) performed an experimental study with a pilot-plant model, using scaled and full-size annuli. The main factors favoring a good mud displacement, such as centralization, pipe movement, optimum flow rate and optimized rheological properties, are generally agreed upon. Yet the integrated mathematical quantifications of those different factors were yet to be formulated. The industry was still relying on a set of “rules” based on these factors to design an efficient mud removal.

This approach persisted for decades. The design rules were proven to be useful and obviously contained a number of physical truths. However, it was difficult to optimize design solely based on them; the fundamental understanding was low and the recommendations made were generally conservative. Later on, when computational capabilities became more accessible, mud displacement started being studied with mathematical models solved numerically. Such early works were performed by (Martin, Latil, & Vetter, 1978) and (Haut & Crook, 1979). Nevertheless, the applications were limited and these simulators were not widely available to the field.

In the 1990s, more comprehensive models were developed (Bittleston, Ferguson, & Frigaard, 2002). Based on this work, a two-dimensional (2D) mud displacement simulator became widely available for the field use. This 2D simulator is now a standard in the industry. Nonetheless, because of the growing complexity of well geometries, some of its limitations started to show.

First, the simulation workflow only considers fluid displacement in the annulus and neglects what happened while fluids travelled down the pipe. The assumption is that different fluids are perfectly separated inside the casing, even after hundreds, or thousands, of meters. In reality, without a mechanical separator, this is physically impossible.

Second, as a matter of performance optimization, the simulator was implemented to simulate only half the annulus, assuming symmetrical flow in the other half. This assumption prevents the determination of azimuthal flow, or flow around the casing, which is of great importance in deviated and horizontal wells with high density-contrast fluids.

Finally, a third limitation is related to the determination of the annulus geometry. The wide spread soft string centralization model used to determine casing eccentricity assumes that standoff is always oriented in the direction of gravity. When a three-dimensional wellbore is considered, it becomes necessary to consider 3D displacements and not just those in the vertical plane. Otherwise, unrealistic mud displacement results can be obtained.

Simulation Workflow

A complex simulation workflow must be followed to obtain cement slurry placement in the annulus at the end of the operation.

The first step consists in running a hydraulics simulation of the operation, together with a temperature simulator. This step accounts for the u-tubing effect (Kelessidis, Rafferty, Merlo, & Maglione, 1994) and provides the position of the free surface in the pipe and the resulting flow rate in the annulus. In addition, the temperature simulation also allows to account for the downhole properties of fluids, which are often temperature and pressure dependent (White, Zamora, & Svoboda, 1997). All these results are needed as input to the displacement simulators.

As a second step, the centralization of the string that will be cemented is determined. As the centralization results depend on the fluids positions within the flow path, the choice is usually made to consider the moment when cement slurry first enters the annulus. This situation also usually corresponds to the most detrimental in terms of standoff, as the apparent weight of the casing string is the highest. It is however possible to determine centralization at any time during cement placement and use these results instead.

All the inputs needed for the two displacement simulators are now available: flow rates in pipe and annulus, free surface position, 3D annulus geometry.

Stiff String Centralization Simulator

The position of the casing inside the well determines the annular geometry used in the fluid displacement simulator presented in section “Fluid Displacement in the Annulus”. Our stiff string centralization model was discussed in detail by (Gorokhova, Parry, & Flamant, 2014) and will only be briefly presented here.

Owing to its extreme length-to-diameter ratio, the tubular string is modeled as an assembly of one-dimensional elastic beams. Each beam is characterized by a uniform cross-section geometry and Hooke elastic constants (Young’s modulus and Poisson’s ratio). Beam elements are individually bounded by two nodes, such that a string of N discrete elements define N+1 nodal points. Local deformations occur under the action of distributed and/or nodal forces, as well as bending and torsion moments. Thus, each node has six degrees of liberty, namely displacement and rotation vectors in three dimensions. String beams are coupled via displacement and rotation continuity at nodes. This implies in particular that bending moments are transmitted from one element to the next along the string. Hence, the model is referred to as “stiff string”, as opposed to the simpler model widely used in the industry, hereafter referred to as “soft string”.

Transverse displacement is constrained by the annular clearance between the casing outer radius and wellbore radius. Hard contact, when it occurs, is handled by a penalty method, through a return force normal to the wellbore wall imposed onto the casing string at contacting nodes. Contact mechanics makes the calculation of displacements nonlinear, as contact points are not known beforehand. The possible presence of bow spring centralizers is modeled by an additional spring force proportional to the local absolute transverse displacement.

Finally, the obtained solution provides the nodal displacement and rotation angles satisfying the balance between internal elastic stresses, buoyancy/gravity forces and contact forces. The relative eccentricity $e(z)$ of the string at a given depth z is computed as the ratio of the absolute transverse displacement to the local annular clearance. This quantity is bounded between 0 (centered casing) and 1 (contact). Standoff ratio is defined as $1 - e(z)$. Standoff orientation is not inferred, as in the soft string model, but computed from the displacement components in each cross-section plane. Axial resolution for typical field cases varies from 1 to 5 meters. Full resolution results are submitted as input to the annular displacement simulator.

Fluid Displacement Physics

In order to predict cement placement along the wellbore, a simulator must solve the downwards flow and displacement of completion fluids along the pipe/casing as well as their upwards flow along the annulus, as depicted in Figure 1.

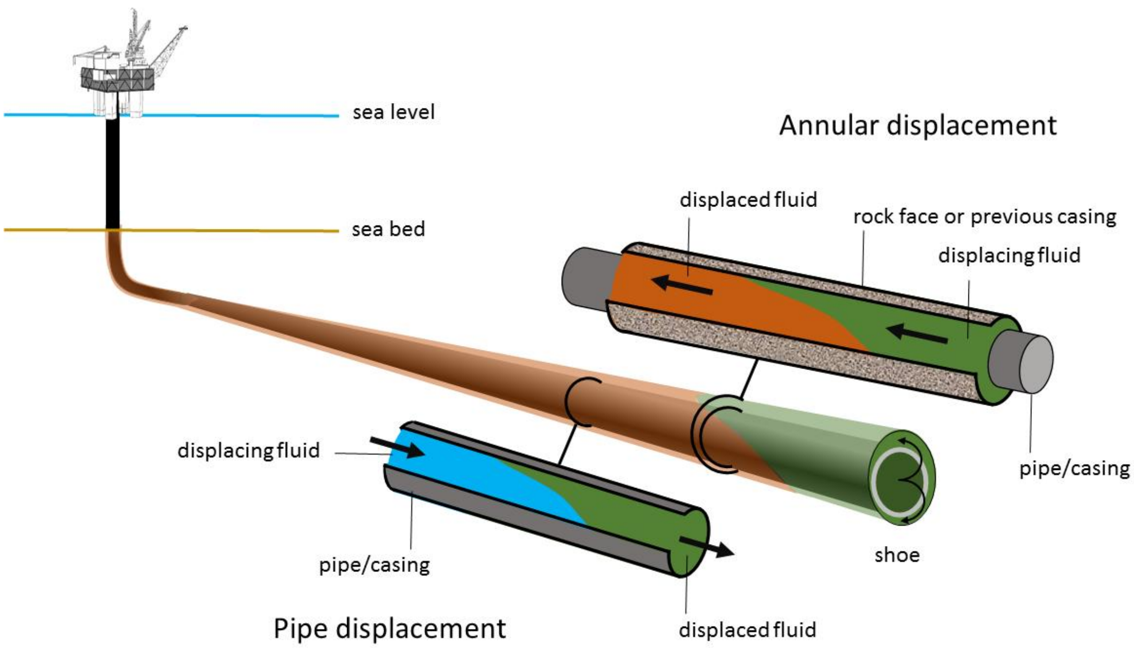

Figure 1: Schematic of the coupling between pipe displacement simulation and annular displacement simulation

Such flows take place along a path of complex and varying geometry and involve multiple physical phenomena which, if not accounted for correctly by the simulator, may lead to poor cementing job design and improper cement placement. Some aspects of the complexity of the displacement physics are listed below.

Annular geometry:

The geometry of the annular space between casing and rock face changes along the wellbore due to wellbore and casing diameters variations. Washouts may also be present. Very importantly, casing centralization and orientation is never uniform. These factors lead to the creation of preferential flow paths, i.e. wider annular gap regions, which may occur at any azimuth around the wellbore (Haut & Crook, 1979). With such paths, the risk of bypassing the fluids on the narrower parts of the annulus increases.

Casing movement:

It has been observed by some (McLean, Manry, & Whitaker, 1967) (Lee & Dorge, 1983) (Hyatt & Partin, 1984) (Bittleston & Guillot, 1991) (Tardy & Bittleston, 2015) that moving the casing while pumping may improve cement zonal coverage and mud circulation. The drag exerted by the moving casing may help remove trapped mud and fluidize gelled fluids.

Viscous forces:

Most muds and slurries exhibit a yield-stress, a gel strength and a shear-dependent rheology (Livescu, 2012). Un-yielded mud may be by-passed and form a channel along the narrow part of the annulus. Adverse friction factor ratios may also lead to mud by-pass. When a less viscous fluid displaces a more viscous one, viscous fingering may occur and lead to poorly swept zones (McLean, Manry, & Whitaker, 1967).

Buoyancy forces:

A denser fluid on top of a lighter one is not a stable situation. When this situation arises, Kelvin-Helmholtz instabilities may develop (Tardy & Bittleston, 2015). As for viscous fingering, buoyancy driven axial flow instability may be detrimental to the efficient displacement of fluids. However, such flow instabilities may occur not only axially but also azimuthally. Buoyancy driven azimuthal flow instabilities have been observed (Tehrani, Bittleston, & Long, 1993) and simulated (Tardy & Bittleston, 2015) and are believed to promote better mud removal. It is often advised to use a density hierarchy when pumping cement through the annulus whereby the wash/spacer is denser that the initially present mud, and the slurry denser than the wash/spacer, in order to prevent axial buoyancy driven fingering (McLean, Manry, & Whitaker, 1967) (Tehrani, Bittleston, & Long, 1993). However, before going up the annulus, the fluids flow downwards in the pipe. There, the hierarchy is reversed and may lead to fluid segregation, or stratification, and by-passing prior to reaching the shoe when wiper plugs are not used. Thus, it is also important to model fluid displacement accurately in the pipe.

The above factors must be accounted for by the simulator to generate scenarios as realistic as possible. The displacement simulator used in this study has two components: the pipe displacement simulator and the annular displacement simulator as schematically illustrated in Figure 1. The two simulators are coupled as they exchange fluid at the shoe. Any fluid leaving the pipe at the shoe enters the annulus and vice-versa.

For both simulators, the fluid rheology is assumed to follow the Herschel-Bulkley model (Livescu, 2012).

$$\tau = \tau_y + \kappa\dot{\gamma}^n \#(1)$$

τ is the shear stress, $\dot{\gamma}$ the shear rate, τ_y the yield stress, κ the consistency index and n the power-law exponent. Such fluid remains solid-like and static until shear stress τ exceeds τ_y. Muds with larger τ_y may give rise to static unswept mud channels along the narrow side of the annulus. Gel Strength is also accounted for by assuming that until yielded for the first time, the effective yield-stress of a fluid is its gel strength. This is mostly relevant for the mud initially present in the annulus. At present, fluid properties are assumed to be independent of pressure and temperature.

Fluid Displacement in Pipe or Casing

The pipe/casing's inside is modeled as a series of cylindrical tubes of varying diameters. The pipe/casing trajectory is defined by the centralization simulator for a given hole-survey and casing-string. Both pipe/casing deviation angles and pipe/casing azimuths are calculated, as represented in Figure 2, and simulated during flow simulations as they may impact fluid distribution along the pipe/casing.

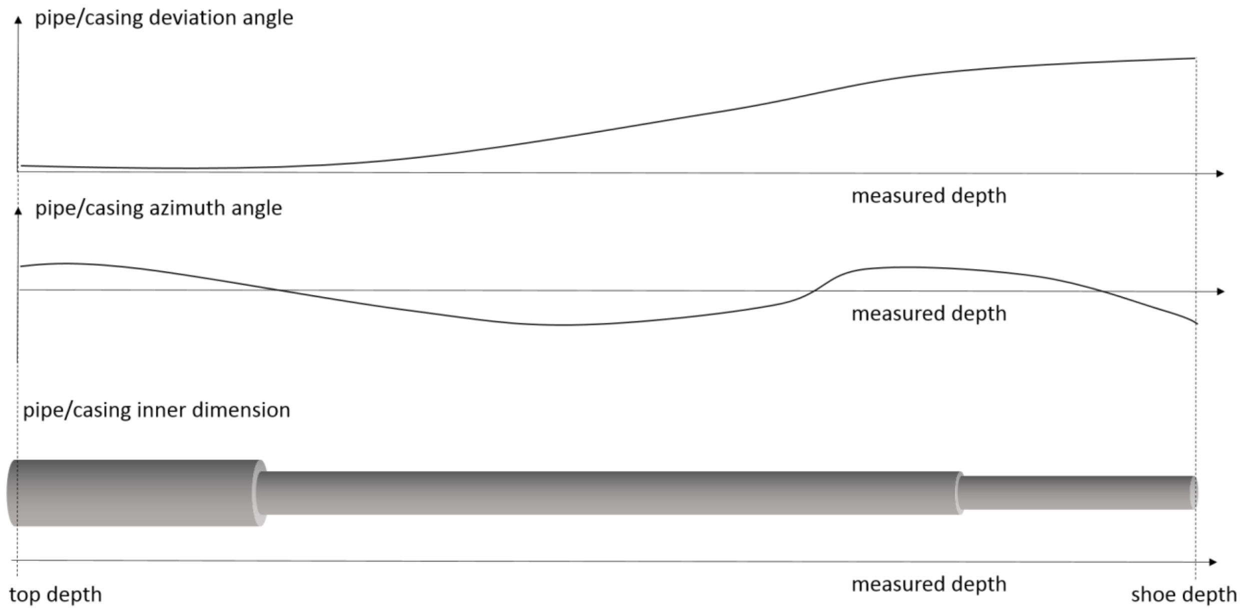

Figure 2: Pipe/casing geometrical parameters for flow simulations. Top: deviation angle. Center: Azimuth angle. Bottom: Inner diameter

The model assumes that the flow may be locally laminar or turbulent. Where laminar, the fluid-fluid displacement pattern may be concentric or segregated depending on the effect of buoyancy forces (see Figure 3 and Figure 4). Concentric displacement patterns occur when buoyancy forces are not sufficient to segregate the fluids and prevent viscous forces to force the displacing fluid to flow preferentially in the region of the pipe center. With sufficiently large buoyancy forces, the lighter (denser) fluid tends to occupy the upper (lower) part of the pipe, leading to a stratified displacement pattern, as shown in Figure 4. Additionally, the model also detects the onset of laminar flow instability such as the Kelvin-Helmholtz (KH) and the roll-wave (RW) instabilities which may occur at the fluid-fluid interfaces as shown in Figure 5. KH instabilities may occur where there is a velocity difference across the interface between two fluids. RW instabilities occur when a fluid sheet experiences variations in friction, causing flow to re-arrange and, eventually form a local fluid buildup. When these instabilities occur, the fluids mix and a homogenous mixture is generated, similar to that observed in turbulent flow where the fluids mix due to flow velocity fluctuations. Once mixed, fluids do not segregate back to concentric and/or stratified flow, even under laminar flow conditions. One of the pipe/casing model output is the volume fraction of each fluid at the shoe at all times. This information is transferred to the annular displacement model that takes over the fate of the fluids during their upwards flow.

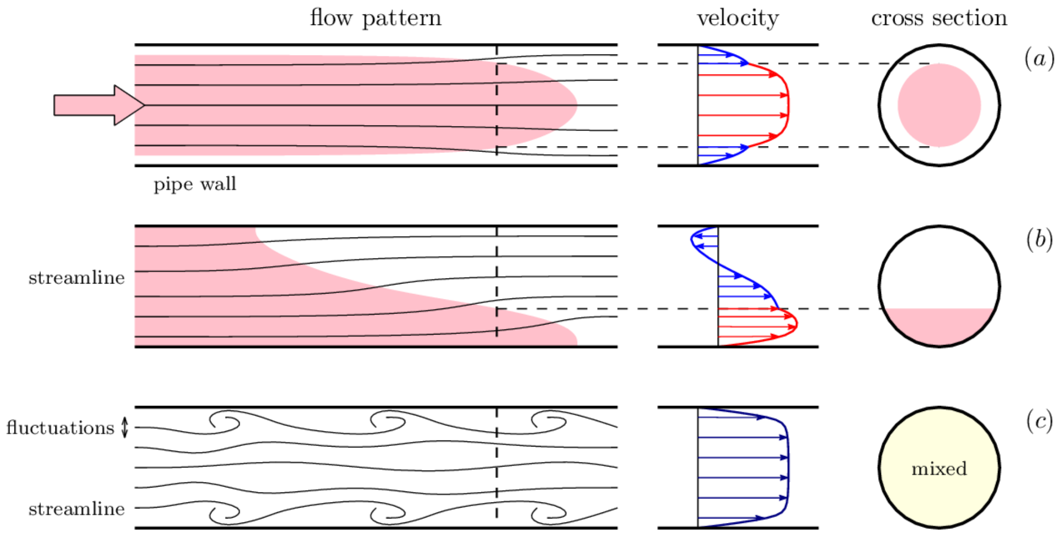

Figure 3: Schematic representation of the laminar and turbulent flow regimes used in the pipe displacement simulator. (a), laminar concentric; (b), laminar segregated; (c), turbulent. The turbulent velocity profile represents the mean flow, in which time/space fluctuations are averaged out.

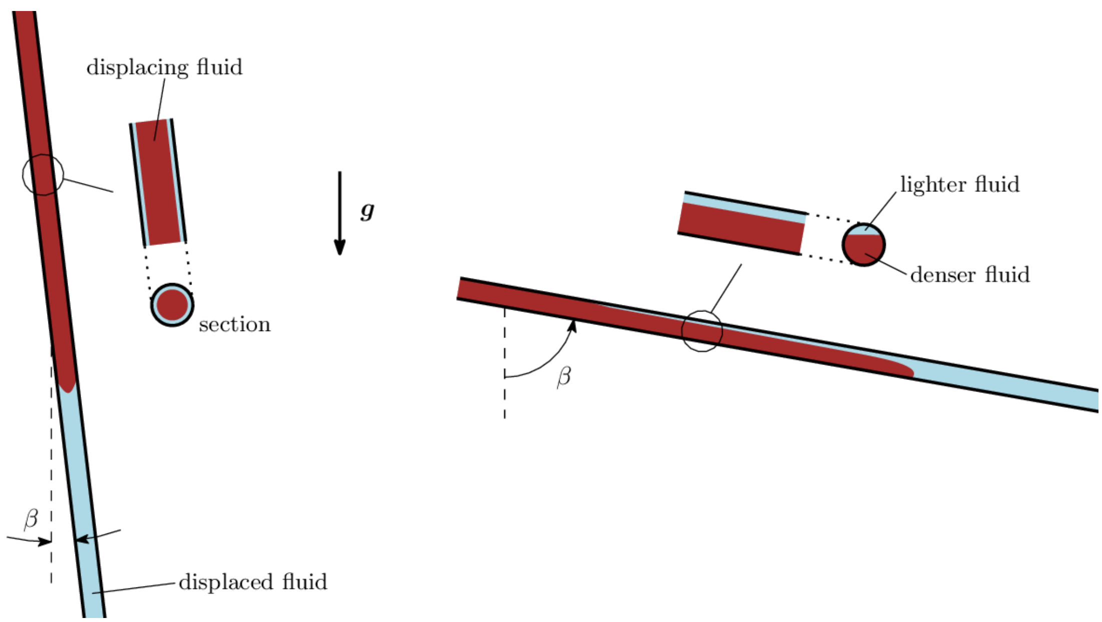

Figure 4: Laminar separated flow types: left, concentric for lower azimuthal buoyancy effects; right, segregated for larger azimuthal buoyancy effects.

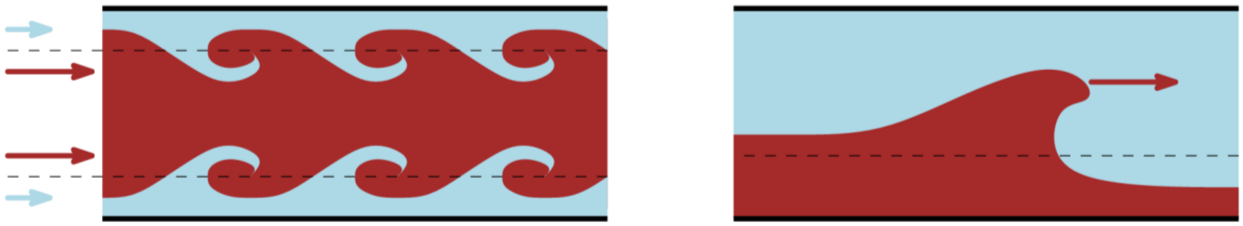

Figure 5: Laminar flow instabilities for pipe displacement flows. Left: Kelvin-Helmholtz. Right: roll-wave

Fluid Displacement in the Annulus

The annular gap width varies significantly along the wellbore, both axially and azimuthally. Such variations give rise to preferential flow paths and must be captured as accurately as possible. A typical simulation grid is shown in Figure 6. Prior to running the displacement calculation, the simulator analyses the geometrical variations of the annulus along the wellbore: standoff magnitude, standoff orientation, inner and outer diameters, wellbore deviation angle and azimuth. The axial grid spacing is automatically adjusted to capture all the details of the actual annular geometry for maximum accuracy as illustrated in Figure 7.

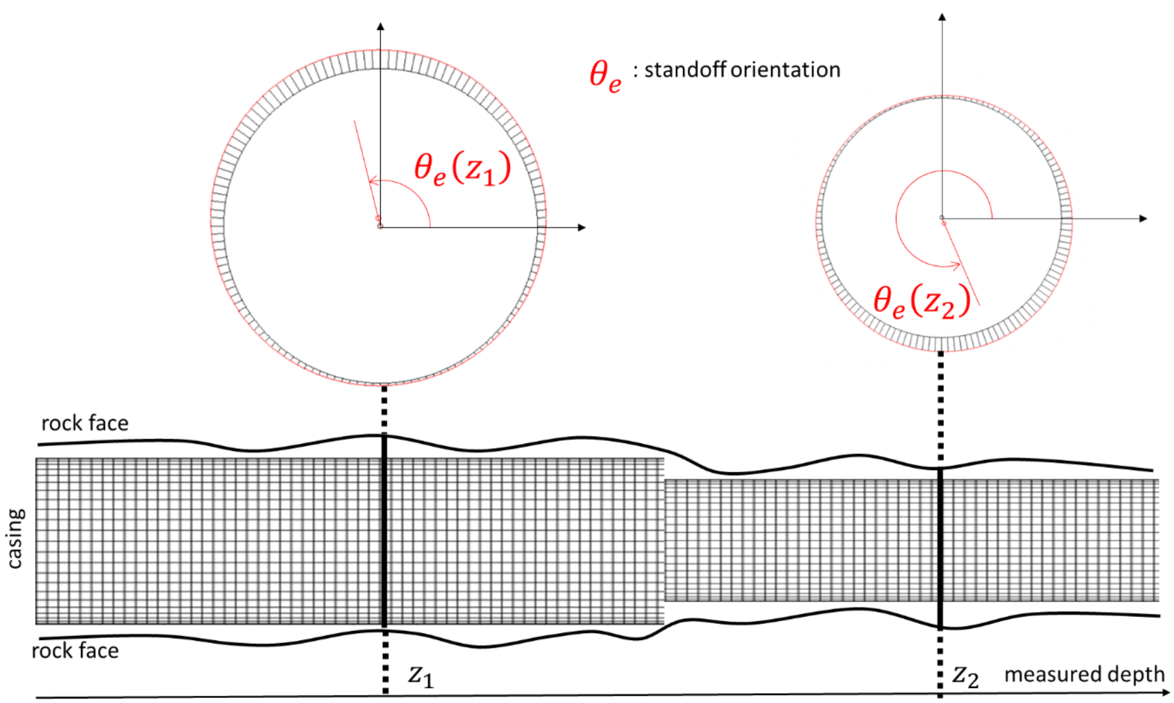

Figure 6: Example of numerical grid used by the annular displacement simulator. Grid projected on casing outer wall with casing axis taken as reference axis: casing standoff becomes rock face standoff.

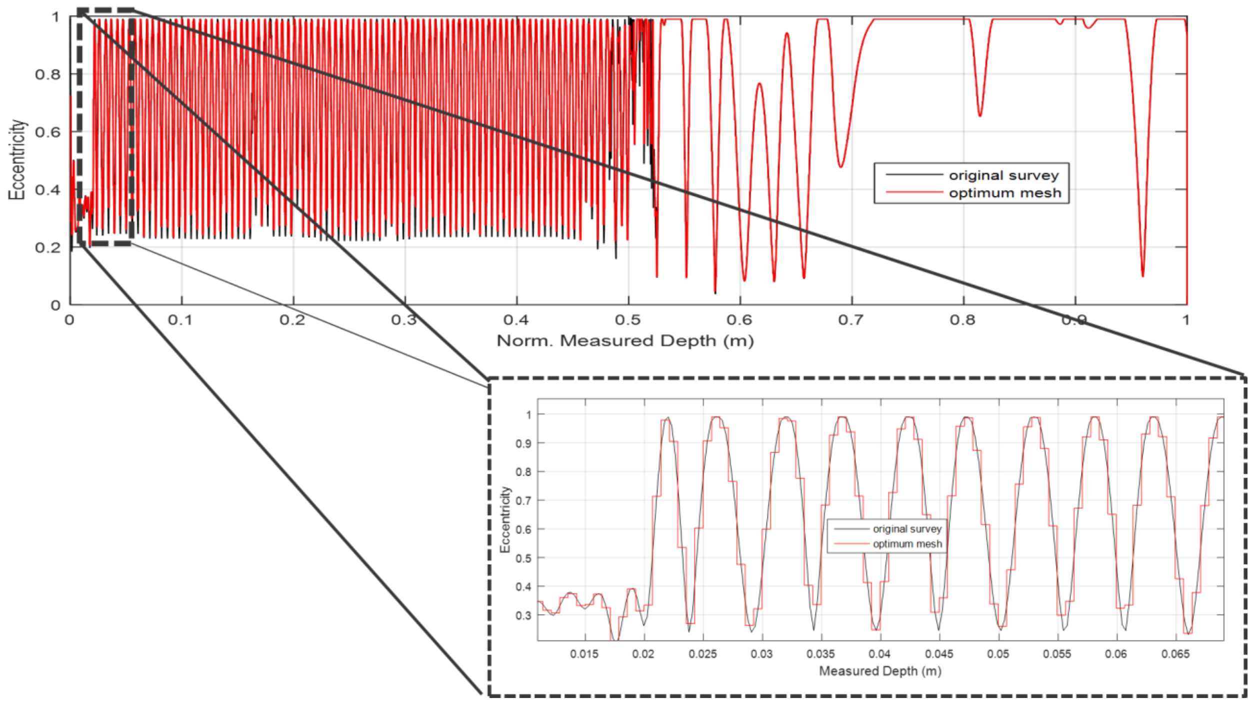

Figure 7: Example of automatic axial discretization for the annular displacement simulator to capture annular geometry as accurately as possible. Here the casing eccentricity, $\boldsymbol{e}$, ($\boldsymbol{e} = (\boldsymbol{STO} - \mathbf{100})/\mathbf{100}$), is used to determine optimum axial mesh size.

The models of the annular displacement simulator are described in details in (Tardy & Bittleston, 2015). As a summary, we report the main features and assumptions here. The simulator assumes that fluids' rheology follows the Herschel-Bulkley model from equation (1). They flow and displace each other depending on the balance of buoyancy forces, viscous forces and the actual annular geometry. Casing rotation and reciprocation is also accounted for. This feature has proven very useful in showing enhanced mud removal while rotating the casing during cement pumping. Unlike previous work (Bittleston, Ferguson, & Frigaard, 2002) (Pelipenko & Frigaard, 2004), flow symmetry is not assumed, standoff orientation may take any value (see Figure 6), and the model lets azimuthal buoyancy effects (such as azimuthal flow instabilities) develop fully without unphysical symmetry (Tardy & Bittleston, 2015). Simulations have shown that allowing full development of azimuthal flow may lead to less pessimistic mud displacement predictions.

The annular flow model assumes that the annular gap width is small compared to the wellbore radius. This allows significant simplifications to take place during the resolution of the Navier-Stokes equations in the 2D azimuthal-axial plan as opposed to the actual 3D axial-azimuthal-radial flow, without significant loss of accuracy. Indeed, the gap width radial dimension is not neglected but averaged only. Doing so allows determing only the mean axial and azimuthal velocity components while still providing accurate friction pressures. The main benefit of using this assumption is that the CPU time is very significantly reduced, allowing simulation results to be obtained in a reasonable time while using a high-definition description of the annular geometry, both axially and azimuthally (e.g. variations of the standoff magnitude and orientation).

Unique features of the new annular simulator coupled to stiff string centralization simulator

Unlike the traditional soft string model, the stiff string centralization model couples all simulation points through the transmission of forces and bending moments along the entire casing/pipe string. This structural mechanics approach provides a more realistic prediction of standoff, and alleviates all a priori assumptions on standoff orientation. For example, our centralization engine is able to predict helicoidal buckling when the casing string is subjected to sufficiently large compressive axial forces. Therefore, stiff string centralization results provide a fully three-dimensional annular flow path geometry, in actual three-dimensional well trajectories. As discussed in “Fluid Displacement in the Annulus”, our fluid displacement engine takes into account arbitrarily complex annular geometries, and captures accurately azimuthal flows that may arise from the interplay between buoyancy forces and viscoplastic fluid rheology.

The association of these two simulators thus appears as a powerful modeling tool to assess the efficiency of mud removal, and quality of cement placement in a target zone. Additionally, the pipe flow simulator evaluates the severity of undesired mixing as the various cementing fluids are pumped into the well.

The ability of this novel simulator suite to predict real-life cementing fluid placement is demonstrated with a case study presented in the next section.

Case Study

We are investigating cement placement in the following well: 4829 m measured depth (MD), with a 1600 m long horizontal section at a true vertical depth (TVD) of 3150 m. The shape of the well is presented in Figure 8. The black circles on the casing string are located at the position of the centralizers. The cementing program includes two spacers ahead of a conventional slurry. The top of cement is planned at 1843 m, *i.e.* about 700 m above the heel and in front of a previous casing string.

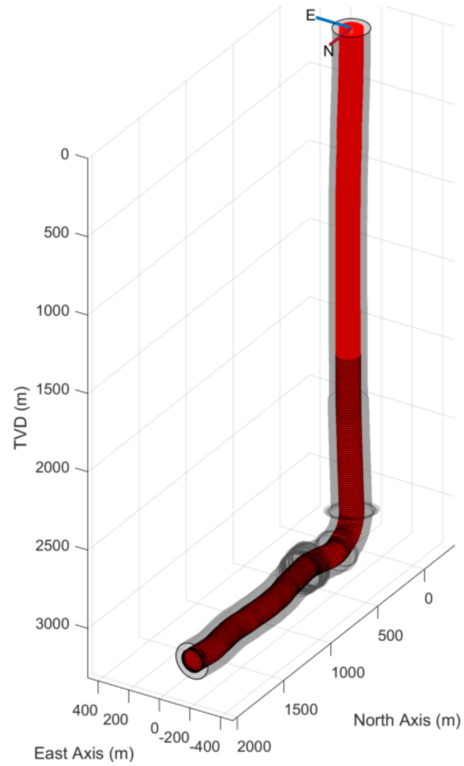

Figure 8: Well Trajectory. The casing is drawn in red, with black circles drawn at the position of centralizers.

After running the hydraulics simulation, the string centralization can be computed. The shape of the string over the centralized interval is presented in Figure 9 and the standoff value vs. depth in Figure 10.

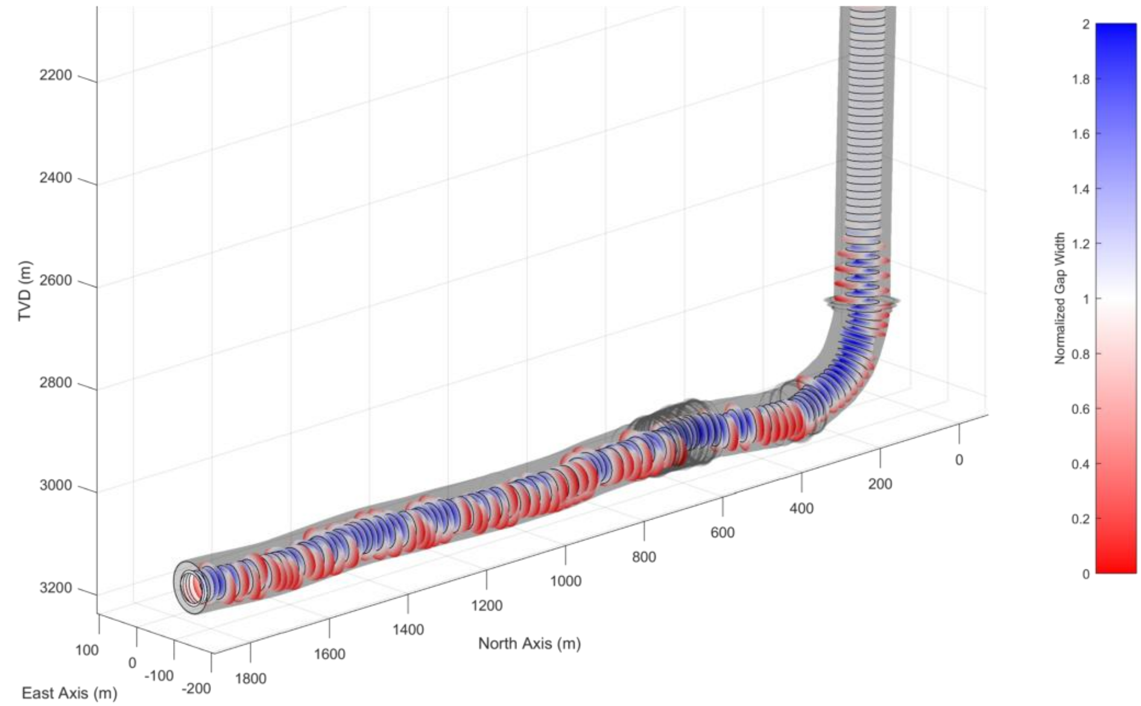

Figure 9: Casing Shape: the color map displays the normalized gap, which varies axially and azimuthally. A value of 0 (red color) corresponds to the casing string touching the wellbore. Diametrically opposite a value of 2 (blue color) will be found. When the string is centered, a value of 1 (white color) is displayed all around. Black circles indicate the positions of centralizers.

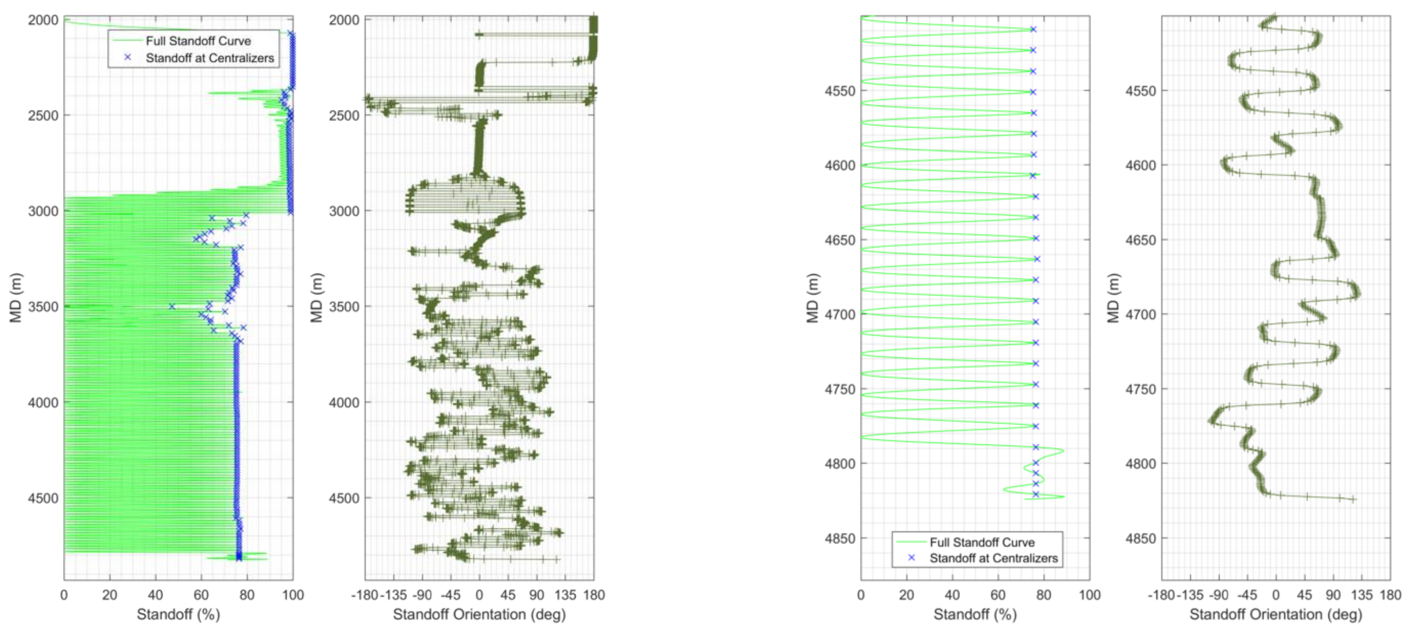

Figure 10: Stiff string standoff results. Full results left, zoomed in section right

In the vertical section of the well, the string is well centralized. Yet despite the high number of centralizers, the standoff achieved in the horizontal part of the well is poor. Although the standoff at centralizers is mostly greater than 75%, in between standoff goes back to 0%, while standoff orientation shows that the string moves from left to right. This effect, akin to buckling, is the result of the axial compressive load of the string in the horizontal part of the well. This compressive load is not taken into account by soft string centralization models, which therefore provide more optimistic results as displayed in Figure 11.

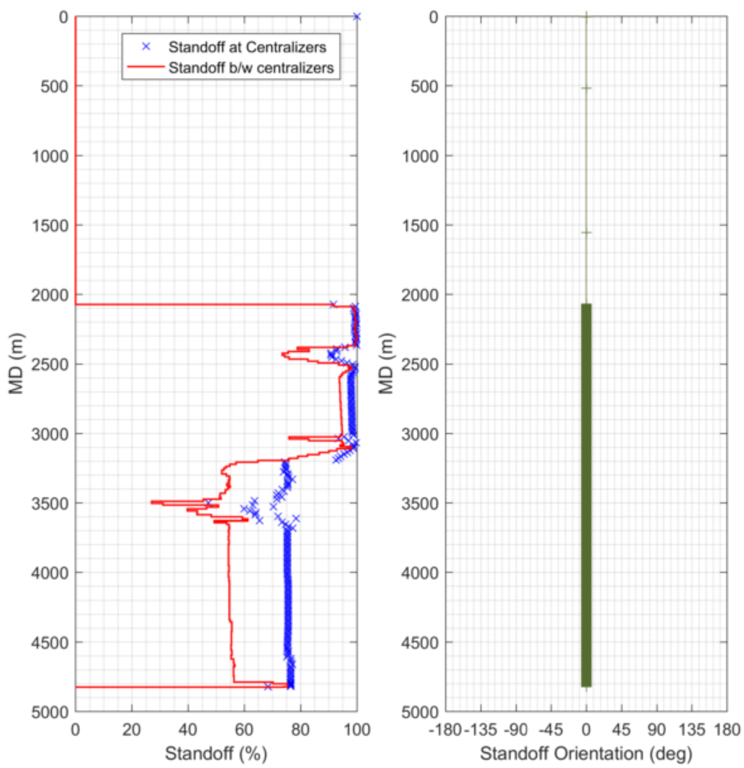

Figure 11: Soft string standoff results

Top and bottom wiper plugs were used to mechanically separate the slurry from the fluids ahead of it and behind it. As a result, the slurry reached the bottom of the casing without having been contaminated while flowing through the pipe. However, this was not the case for the two spacers and Figure 12 provides the fluids concentration in the pipe at the time of the first spacer breakthrough. Unfortunately, the spacers are significantly mixed with each other but also with mud, which will affect their efficiency once in the annulus.

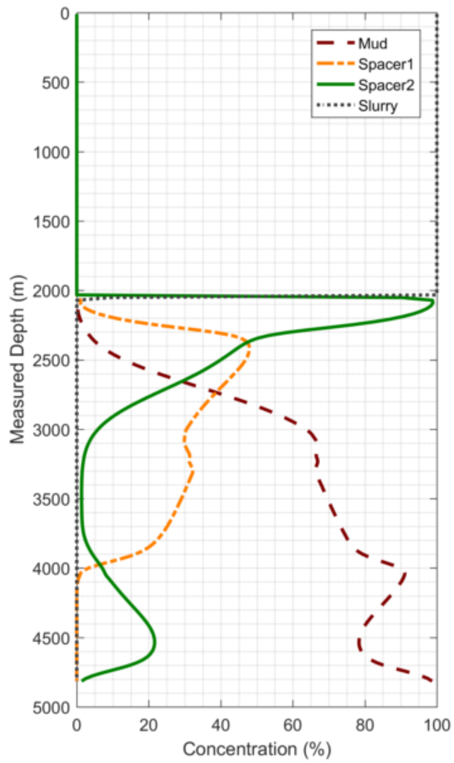

Figure 12: Fluids concentrations in pipe at spacer breakthrough

The results from the previous generation annular displacement simulator, obtained with the centralization soft string results, are presented in Figure 13. Although standoff between centralizers in the horizontal section does not fall below 40%, a large mud channel occupying more than a third of the hole circumference is predicted.

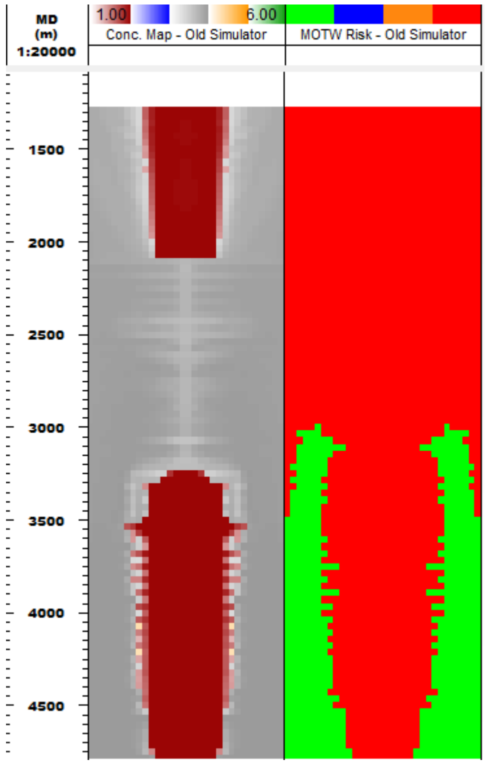

Figure 13: Old simulator cement placement results. On the concentration map, all fluids are assigned a color: gray, brown, orange and green for slurry, mud, first spacer and second spacer respectively. At any point on the map, the color displayed is that of the dominant fluid. The color is then adjusted as a function of concentration via a concentration weighted average between the pure color and white. The Mud On the Wall (MOTW) map evaluates the risk of leaving a mud layer on the casing or wellbore walls. Red = high risk, Green = no risk, Blue and Orange = medium risk.

The new generation annular displacement simulator now takes into account the much richer centralization results obtained with the stiff string model. In addition, it was run with a high axial resolution of 1 m and 64 cells in the azimuthal direction. The results are presented in Figure 14. We would also like to underline here that these results can be obtained in a matter of minutes on standard laptops as used by field personnel, which makes the simulator suitable for day to day engineering work.

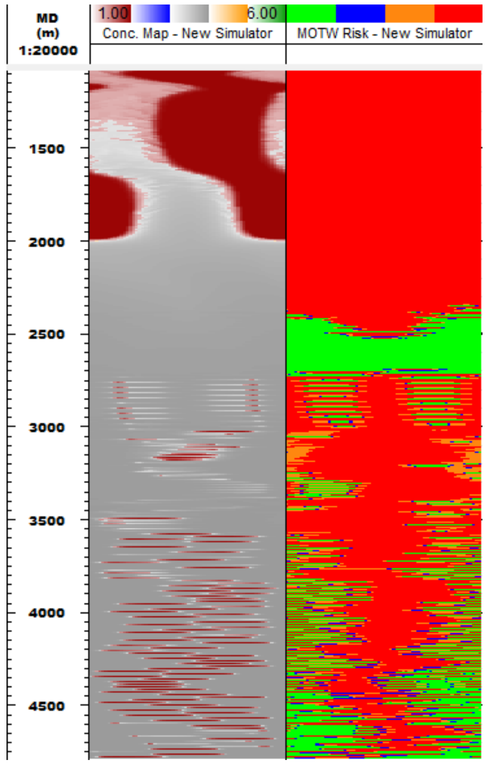

Figure 14: New simulator cement placement results. The color scales are the same as on Figure 13.

Figure 15 shows a close-up view on a short section of the annulus to highlight the details of the simulation results and compare it to the results from the old simulator. Instead of a large and uniform mud channel, the new model predicts that pockets of mud remain un-displaced in the low standoff parts of the annulus. As standoff is not oriented towards the bottom of the hole, these pockets are distributed all around the hole circumference. These results illustrate well the role of azimuthal flows in mud displacement. The fluids densities are respectively 1750 kg/m3, 1800 kg/m3 and 1890 kg/m3 for the mud, spacers, and cement slurry. This density hierarchy is sufficient to trigger buoyancy-driven azimuthal flows for the spacers, which then successfully remove mud except in the areas of near-zero standoff. Similarly, the slurry then successfully displaces the spacers ahead of it.

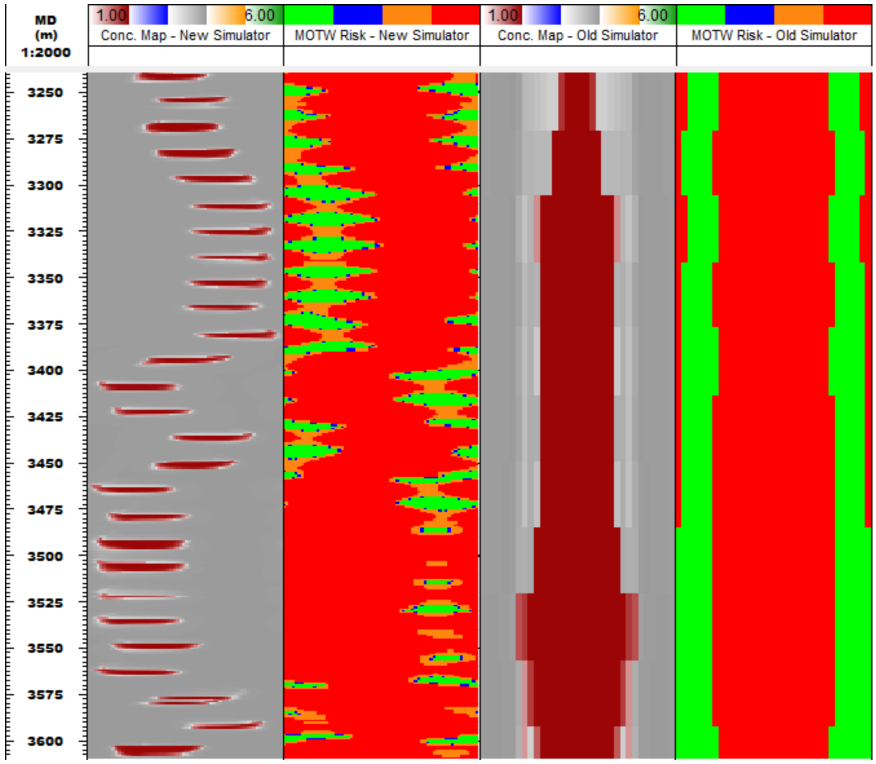

Figure 15: New vs. old simulator cement placement results over a short interval. The color scales are the same as on Figure 13.

An ultrasonic log was run after cement placement. To help with interpretation, the expected acoustic impedances for the fluids and cement are presented in Table 1.

MRay	Min	Expected	Max
Mud	1.2	1.7	2.2
Slurry	2.2	2.7	3.2
Cement	5.1	6.0	6.9

Table 1 – Expected acoustic impedances in MRay

Unfortunately, it was not possible to log deeper than 3230 m, *i.e.* still in the heel of the well, at a maximum inclination of about 70 deg. The simulation and log results will therefore be compared over the 1100 m – 3200 m depth range. Figure 16 provides the overall comparison. Note that the log has not been compensated for the orientation of the tool, and therefore we cannot expect to get an azimuthal correspondence between the log and the concentration map. The effective top of cement is consistently predicted by both the simulation and the log at 2000 m.

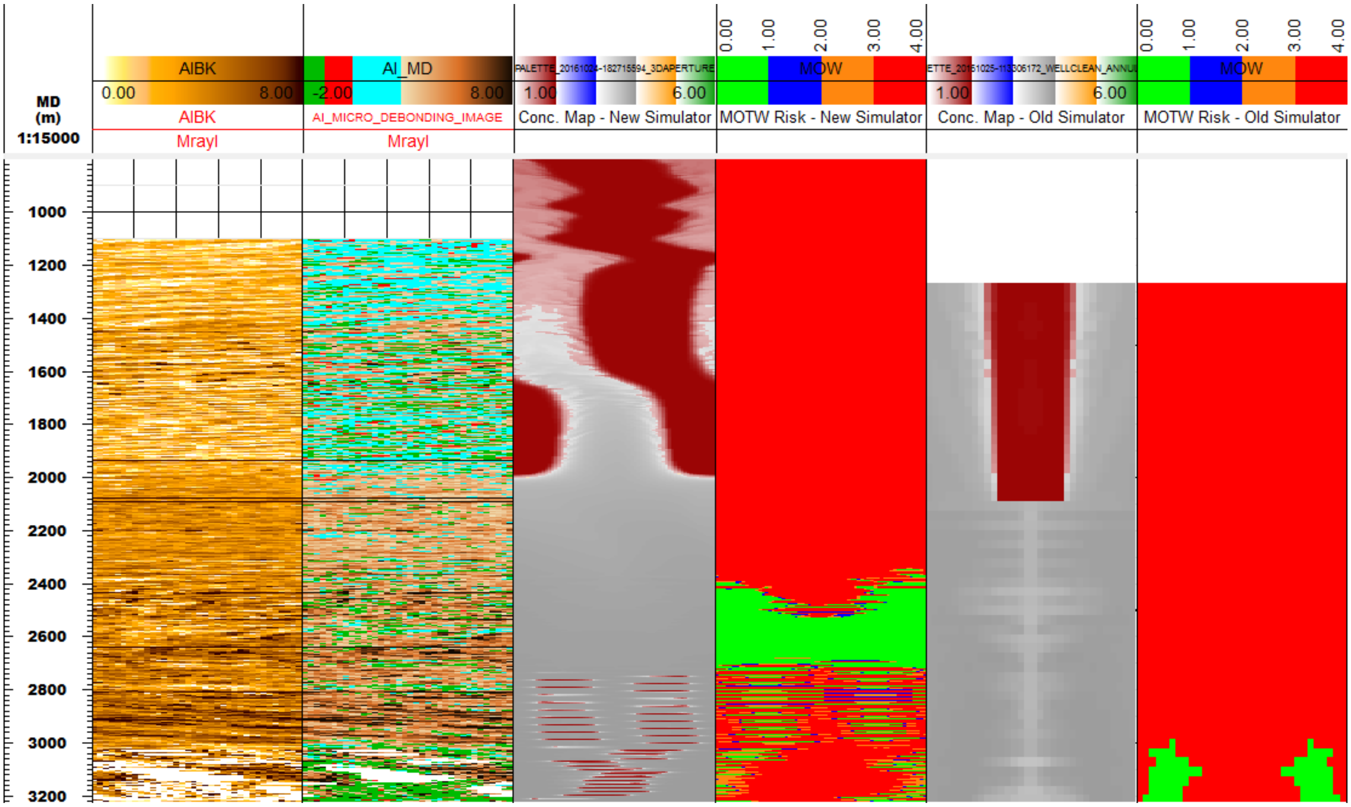

Figure 16: Placement simulation results vs. ultrasonic log

At shallower depths, a liquid channel is seen on the log as well as on the concentration map as highlighted in Figure 17. The maximum acoustic impedance is around 5 Mray, which is consistent with the presence of cement. Nonetheless, this value is on the low side (Table 1), which may be the result of slurry contamination. Indeed, the slurry concentration map shows that the slurry is not pure, and is instead a mixture of 75% slurry, and 25% mud and spacer.

While still in the vertical section, competent cement is found deeper in the well, as shown on Figure 18. The average acoustic impedance is around 5 MRay. The log does show that the cement is somewhat patchy, which can be the result of slurry contamination as the simulation shows that the slurry contains about 5% of mud and spacers. This could also be related to an un-displaced mud layer on the wall of the casing, as indicated by the high mud on the wall risk.

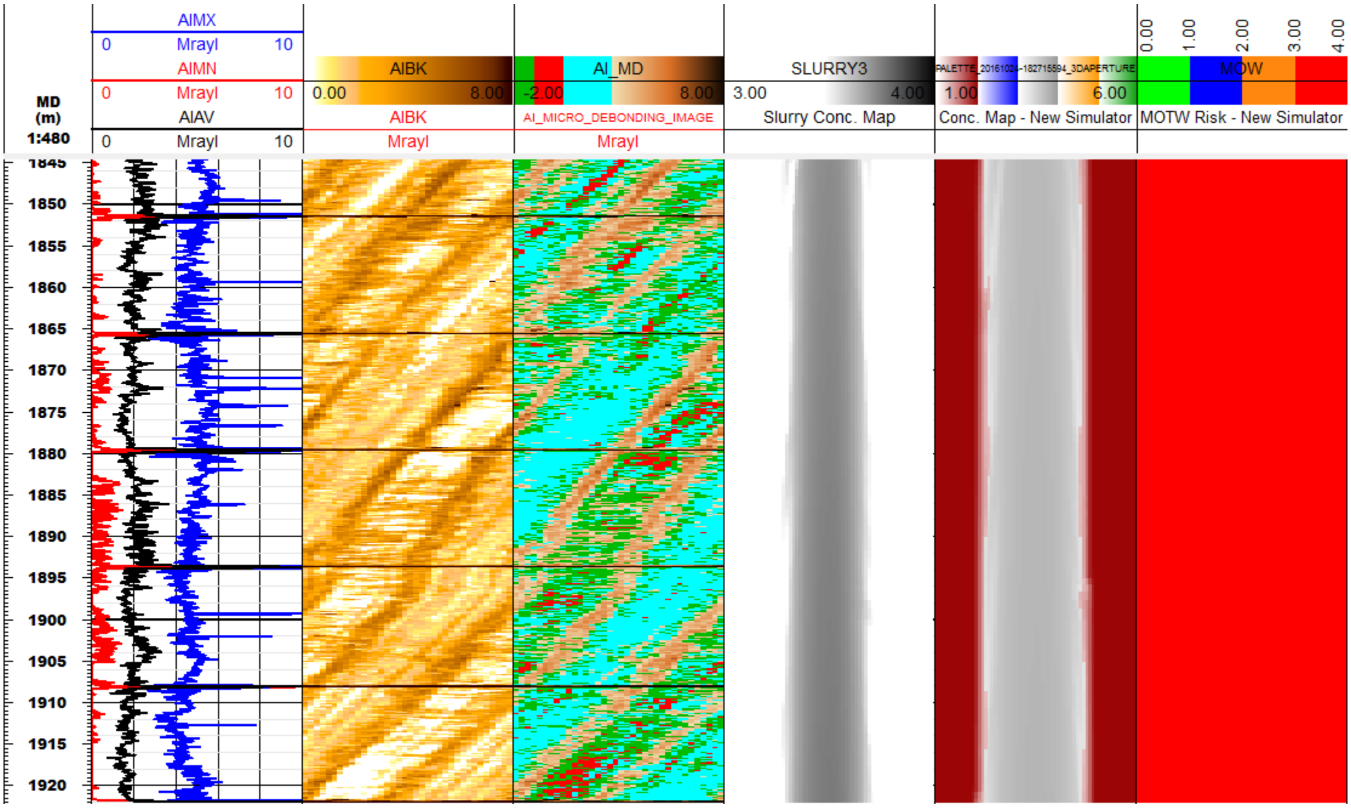

Figure 17: Placement simulation results vs. ultrasonic log above top of cement. The slurry concentration map provides a more quantitative view of the slurry concentration. The color scale is such that concentration less than 50% shows as white and 100% concentration shows as black, with shades of gray in between.

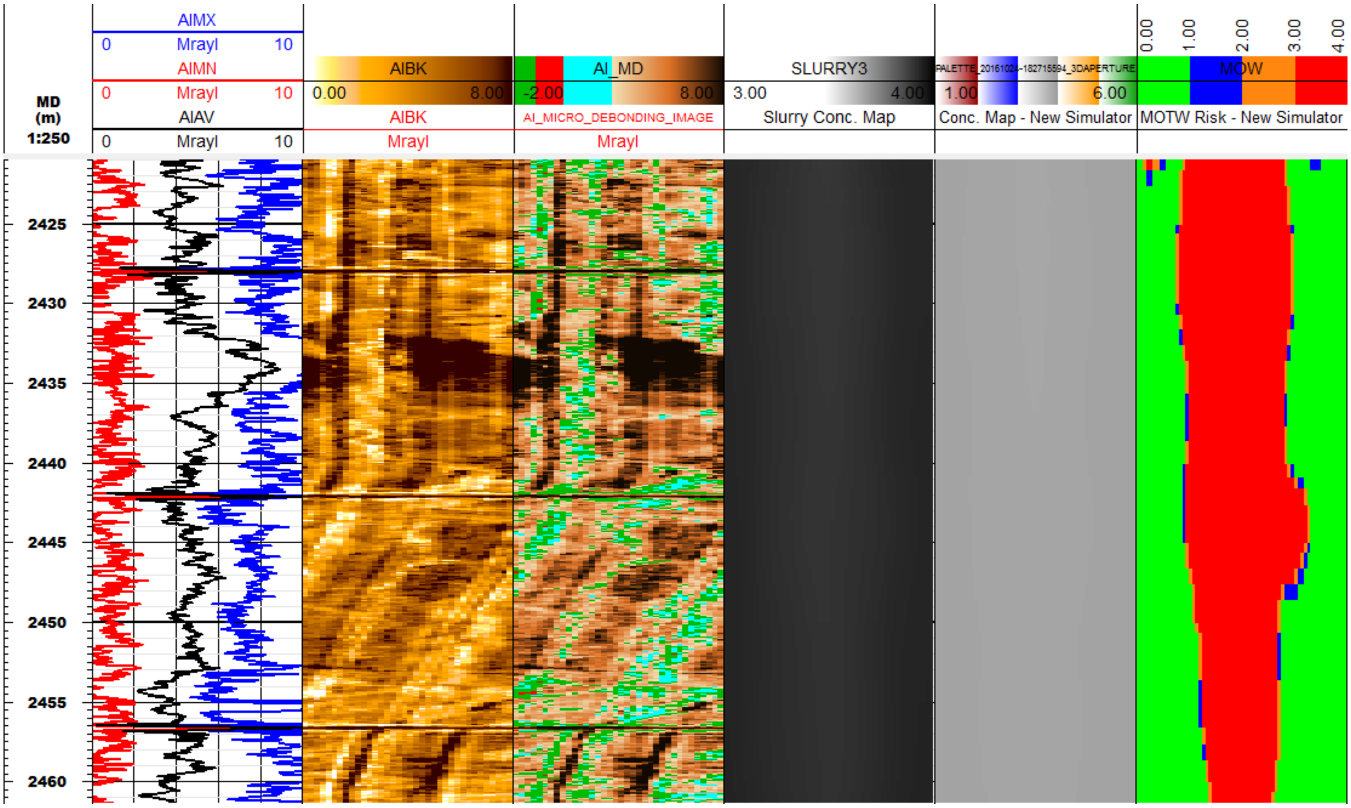

Figure 18: Placement simulation results vs. ultrasonic log below the top of cement

Figure 19 shows that the cement qualities deteriorate in the heel of the well. The log reveals pockets of liquid, as also visible in simulated concentration maps.

Overall the results from the new simulator show very good agreement with the ultrasonic log and highlight features that the previous generation simulator was not capable of determining.

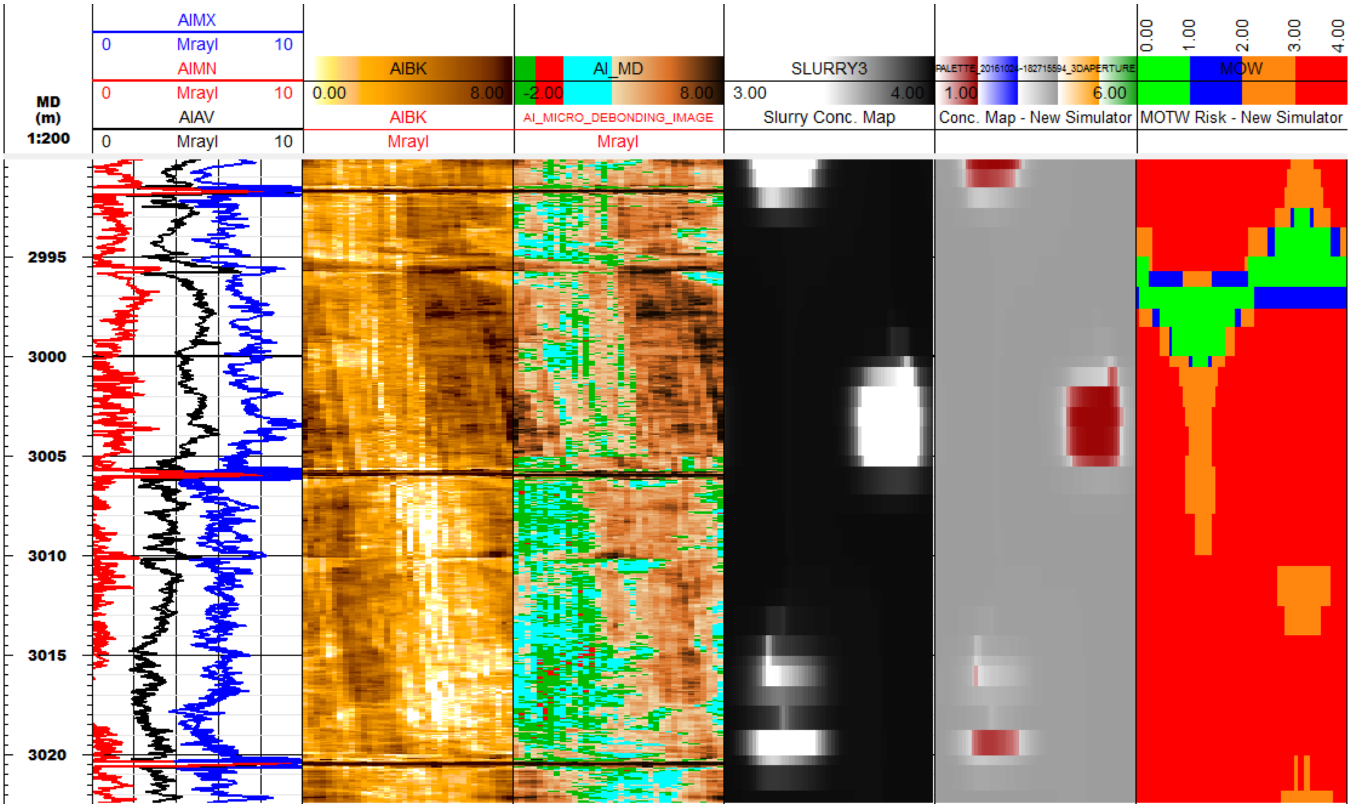

Figure 19: Placement simulation results vs. ultrasonic log in the heel

Conclusion

The new simulation workflow, which includes three novel simulators for centralization, pipe and annular displacement, was successfully applied to a horizontal well. The simulation results provide unprecedented details compared to the previous generation simulators and compare well with the cement evaluation acoustic log.

References

Bittleston, S., & Guillot, D. (1991). Mud removal: Research improves traditional cementing guidelines. *Oilfield Review, 3,* 44-54.

Bittleston, S., Ferguson, J., & Frigaard, I. (2002). Mud removal and cement placement during primary cementing of an oil well - Laminar non-Newtonian displacements in an eccentric annular Hele-Shaw cell. *Journal of engineering Mathematics, 43 (2-4)*, pp. 229-253.

Gorokhova, L., Parry, A. J., & Flamant, N. C. (2014, February). Comparing Soft-String and Stiff-String Methods Used to Compute Casing Centralization. *SPE Drilling & Completion, 29*, 106-114. doi:10.2118/163424-pa

Haut, R. C., & Crook, J. C. (1979). Primary Cementing: The Mud Displacement Process. *54th Annual Fall Technical Conference of the SPE of AIME, SPE 8253.* Las Vegas, Nevada.

Hyatt, C. R., & Partin, M. H. (1984). Liner Rotation and Proper Planning Improve Primary Cementing Success. *SPE Deep Drilling and Production Symposium.* Society of Petroleum Engineers (SPE). doi:10.2118/12607-ms

Jones, P. H., & Berdine, D. (1940, 1). Oil-Well Cementing. American Petroleum Institute.

Kelessidis, V. C., Rafferty, R., Merlo, A., & Maglione, R. (1994). Simulator models U-tubing" to improve primary cementing.

Lee, W. T., & Dorge, W. D. (1983). Cementing-Simultaneous Rotation-Reciprocating Technique (ROTO-TEK System). *IADC/SPE Drilling Conference.* Society of Petroleum Engineers (SPE). doi:10.2118/11419-ms

Livescu, S. (2012). Mathematical modeling of thixotropic drilling mud and crude oil flow in wells and pipelines—A review. *J. Petroleum Sci. Engng*, *98–99*, 174-184. doi:10.1016/j.petrol.2012.04.026

Martin, M., Latil, M., & Vetter, P. (1978). Mud Displacement By Slurry During Primary Cementing Jobs - Predicting Optimum Conditions. *SPE Annual Fall Technical Conference and Exhibition.* Society of Petroleum Engineers (SPE). doi:10.2118/7590-ms

McLean, R., Manry, C., & Whitaker, W. (1967, February). Displacement Mechanics in Primary Cementing. *Journal of Petroleum Technology, 19 (2),* pp. 251-260.

Pelipenko, S., & Frigaard, I. A. (2004). Mud removal and cement placement during primary cementing of an oil well – Part 2; steady-state displacements. *J. Engng Math.*, *48*, 1-26. doi:10.1023/B:ENGI.0000009499.63859.f0

Tardy, P. M., & Bittleston, S. H. (2015). A Model for Annular Displacements of Wellbore Completion Fluids Involving Casing Movement. *J. Pet. Sci. Eng.*, *126*, 105-123. doi:10.1016/j.petrol.2014.12.018

Tehrani, M. A., Bittleston, S. H., & Long, P. J. (1993). Flow instabilities during annular displacement of one non-Newtonian fluid by another. *Exp. Fluids*, *14*, 246-256.

White, W. W., Zamora, M., & Svoboda, C. F. (1997, sep). Downhole Measurements of Synthetic-Based Drilling Fluid in an Offshore Well Quantify Dynamic Pressure and Temperature Distributions. *SPE Drilling & Completion*, *12*, 149-157. doi:10.2118/35057-pa

Zuiderwijk, J. J. (1974). Mud Displacement In Primary Cementation. *SPE European Spring Meeting.* Society of Petroleum Engineers (SPE). doi:10.2118/4830-ms

CV – Santiago Pablo Baggini Almagro

Chemical Engineer, Universidad Nacional de Córdoba

Cementing Technical Manager

CV – Nicolas Flamant

General Engineering, Ecole Nationale Supérieure des Mines de Nancy (*France*)

Project Manager - Cementing Instrumentation & Modeling Projects

CV – Candra Sutama

Chemical Engineering, Gadjah Mada University (*Indonesia*)

Product Champion- Cementing Software & Modeling